Neoplasia • Vol. 6, No. 5, September/October 2004, pp. 603–610 603

www.neoplasia.com

Activation of the Erk Pathway Is Required for TGF-β1–Induced EMT *In Vitro*[1]

Lu Xie, Brian K. Law, Anna M. Chytil, Kimberly A. Brown, Mary E. Aakre and Harold L. Moses

Vanderbilt-Ingram Cancer Center, 2220 Pierce Avenue South, Vanderbilt University, Nashville, TN 37232, USA

Abstract

Transforming growth factor-β1 (TGF-β1) can be tumor-suppressive through the activation of the Smad-mediated signaling pathway. TGF-β1 can also enhance tumor progression by stimulating epithelial-to-mesenchymal transition (EMT) through additional pathways. EMT is characterized by the acquisition of a fibroblast-like cell morphology, dissolution of tight junctions, disruption of adherence junctions, and formation of actin stress fibers. There is evidence linking the activation of mitogen-activated protein kinase pathways to the induction of TGF-β1–mediated EMT. However, the role of Erk in the induction of TGF-β1–mediated EMT remains unclear. TGF-β1 treatment of normal murine mammary gland (NMuMG) epithelial cells resulted in increased gene expression of Ras, Raf, MEK1/2, and Erk1/2, as shown by microarray analysis and real-time polymerase chain reaction. Upon 24 and 48 hours of treatment with TGF-β1, NMuMG and mouse cortical tubule (MCT) epithelial cells underwent EMT as shown by changes in cell morphology, delocalization of zonula occludens-1 and E-cadherin from cell–cell junctions, and formation of actin stress fibers. TGF-β1 treatment also resulted in increased levels of phosphorylated Erk and Erk kinase activity. Treatment with an MEK inhibitor, U0126, inhibited increased Erk phosphorylation and kinase activity, and blocked TGF-β1–induced EMT in both cell lines. These data show that TGF-β1 induces the activation of the Erk signaling pathway, which is required for TGF-β1–mediated EMT *in vitro*.

Neoplasia (2004) **6**, 603–610

Keywords: TGF-β, Erk, pathway, EMT, *in vitro*.

Introduction

Transforming growth factor-β1 (TGF-β1) signaling controls many cellular processes, including cell proliferation, differentiation, apoptosis, and epithelial-to-mesenchymal transition (EMT) [1]. TGF-β1 signals through cell surface serine–threonine kinase type II (TβRII) and type I (TβRI) receptors. TGF-β1 binding to TβRII triggers TβRI association with TβRII. TβRII phosphorylates and activates TβRI, which phosphorylates receptor-associated (RA) Smads (Smad2 and Smad3). RA-Smads bind Smad4 and translocate to the nucleus, where they regulate the transcription of target genes [2] . Smad-dependent signaling is required for the antiproliferative activity of TGF-β1 [3], which mediates TGF-β1 tumor-suppressive effects in early stages of tumorigenesis. However, Smad-independent TGF-β1 signaling has been demonstrated, involving the mitogen-activated protein kinase (MAPK) pathways, including Jun N-terminal kinase (JNK) [4–6], extracellular signal–regulated kinase (Erk) [7], and p38 mitogen–activated protein kinase (p38MAPK) [8]. Phosphatidyl inositol 3-kinase–Akt (PI3-Akt) and RhoA pathways were also reported to be activated by TGF-β1 signaling [9,10]. These pathways may be more closely associated with TGF-β1 induction of EMT and may promote tumor cell invasion and metastasis.

The differentiated epithelial phenotype is characterized by structural and functional polarization of the cell surface, and formation of a junctional complex that mediates strong intercellular adhesion and polarity [11]. E-cadherin, the major component of adherens junctions, forms homophilic contacts between neighboring cells. Tight junctions consist of a multiprotein complex, including the protein zonula occludens-1 (ZO-1), that link tight junctions to microfilaments [12]. EMT is a complex process associated with the loss of this epithelial cell phenotype, dissolution of the junctions containing ZO-1 and E-cadherin, and reorganization of the actin cytoskeleton [9,13,14]. TGF-β1 is a prominent EMT-inducing factor in both normal and pathologic conditions, such as in development of cancer. The induction of EMT by TGF-β1 is associated with the activation of JNK, p38, Erk, PI3k–Akt, and RhoA. However, the precise role of these pathways in the induction of EMT by TGF-β1 is unclear.

Expression profiling analysis is a powerful tool to study the regulation of multiple signaling pathways. Microarray has been utilized to study TGF-β1–mediated EMT [15]; however, this analysis has not been performed on mammary gland epithelial

Abbreviations: TGF-β1, transforming growth factor-β1; EMT, epithelial-to-mesenchymal transition; JNK, Jun N-terminal kinase; Erk, extracellular signal–regulated kinase; p38MAPK, p38 mitogen–activated protein kinase; PI3k, phosphatidyl inositol 3-kinase; NMuMG, normal murine mammary gland; ZO-1, zonula occludens-1; RT-PCR, real-time polymerase chain reaction; MCT, mouse cortical tubule

Address all correspondence to: Harold L. Moses, 691 Preston Building, Nashville, TN. E-mail: hal.moses@vanderbilt.edu

[1]This work was supported by grant nos. CA85492-04 and CA102162 from the National Cancer Institute and the TJ Martell Foundation.

Received 19 March 2004; Revised 27 May 2004.

DOI 10.1593/neo.04241

cells until our previous study [16]. In that study, expression profiling was performed by microarray on mouse mammary gland epithelial cells (NMuMG) that underwent EMT upon treatment with TGF-β1. Interestingly, treatment of NMuMG with TGF-β1 for 1, 6, and 24 hours resulted in increased gene expression of Erk signaling pathway components, including Ras, MEK1/2, and Erk1/2.

Based on the observation that the Erk signaling pathway is activated in NMuMG in response to TGF-β1, we used real-time polymerase chain reaction (RT-PCR) in our current study to confirm the microarray data. Furthermore, the role of the Erk signaling pathway in TGF-β1–induced EMT was investigated using the MEK inhibitor, U0126, in NMuMG cells. Although there is growing interest in TGF-β1–mediated EMT, this is a rare event *in vitro*. To identify alternative cell systems in which to study TGF-β1–induced EMT, 18 established human and mouse cell lines were screened for TGF-β1–induced EMT. Of the cell lines screened, only two underwent TGF-β1–induced EMT: NMuMG and MCT (mouse proximal tubule epithelial cells) [38]. Tubulointerstitial fibrosis is a common end-point of many chronic renal diseases and contributes to the permanent loss of renal function. There is increasing evidence that TGF-β1 plays an essential role in this profibrogenic process. So the role of the Erk signaling pathway in TGF-β1–induced EMT was also investigated in this relevant cell model of MCT. Our data showed that the Erk pathway was required for TGF-β1–induced EMT in NMuMG and MCT, as indicated by the blockage of TGF-β1–induced EMT in both cell lines by U0126.

Materials and Methods

Antibodies and Other Reagents

Porcine TGF-β1 was from R&D System (Minneapolis, MN), prepared in 10 μg/ml stocks in 4 mM HCl. The MEK1/2 inhibitor U0126 (Promega, Madison, WI) was kept as 10 mM stocks in DMSO according to manufacturer's instructions. Antibodies used for immunofluorescence were ZO-1 (Zymed, South San Francisco, CA) and E-cadherin (Transduction Laboratories, Lexington, KY). Texas Red-X phalloidin and Hoechst 33258 were from Molecular Probes (Eugene, OR). The biotin-conjugated secondary antibodies were from Vectastain Elite ABC kits (Vectastain, Burlingame, CA). Streptavidin-conjugated Cy3 was from Sigma (St. Louis, MO). The following antibodies were used for Western blot analysis: phospho-Smad2 (Upstate Biotechnology Inc., Lake Placid, NY); total Smad2/3 (Transduction Laboratories); phospho-Raf1, total Raf1, phospho-MEK1/2, total MEK1/2, phospho-Erk, and total Erk (Cell Signalling Technology, Beverly, MA); and β1-actin (Santa Cruz Biotechnology, Santa Cruz, CA). Secondary horseradish peroxidase–conjugated anti–mouse and anti–rabbit antibodies were purchased from Dako (Carpinteria, CA). ECL Western Blotting Detection Reagents were purchased from Amersham Biosciences (Piscataway, NJ). The Erk1 (C-16) rabbit polyclonal antibody (Santa Cruz Biotechnology) was used for kinase assays.

Cell Culture and Treatment

NMuMG cells were grown in 10% FBS–Dulbecco's modified Eagle's medium (DMEM) containing 10 μg/ml insulin. MCT cells were grown in 10% FBS–DMEM. Cells were cultured in a humidified atmosphere (5% CO_2) at 37°C until they were 70–80% confluent. All cell culture reagents were from Hyclone (Logan, UT). For each experiment, cells were treated with TGF-β1 (4 ng/ml), TGF-β1 (4 ng/ml) plus U0126 (10 μm), or 10 μm U0126 alone, or left untreated. The treatment times were either 24 or 48 hours depending on the particular assay. Each experiment was conducted at least three times.

Microarray and RT-PCR

Microarray and data analyses were described previously [16]. To verify the data obtained from microarrays, RT-PCR analysis of selected genes was performed. The following primers were designed with primer express software (Applied Biosystems, Foster City, CA) and used for RT-PCR: H-ras (forward) GCAATTTATGCTGCCGAATCTC; H-ras (reverse) CAGCTATGGCATCCCCTACATT; N-ras (forward) AGCAGTGACGATGGCACTCAA; N-ras (reverse) GGCATCAGTGCAGCTTCAAAGT; Raf1 (forward) GAAAGCCATCCACACAGGACA; Raf1 (reverse) TGCCAGTTTTGCACATGGAG; MEK2 (forward) TTGATGAAGGCGTGGTTCATC; MEK2 (reverse) CCAGTGGTGTGTTCAGCTCAGA; Erk1 (forward) GCGTTACATGTGGCAGCTTGA; Erk1 (reverse) TGGAACCCCACCCCATTTT; β1-actin (forward) AGAAAATCTGGCACCACACC; and β1-actin (reverse) GGGGTGTTGAAGGTCTCAAA.

Primers were designed to have similar GC content and melting temperatures. In general, amplicons were between 100 and 150 nucleotides in length. Thermal cycling was performed using an ABI Prism 7700 Sequence Detector (Perkin-Elmer Applied Biosystems, Foster, CA). Data analysis was performed with a Sequence Detector, version 1.7. Total RNA (5 μg) was reverse-transcribed with random primers using the Super Script II (Invitrogen, Carlsbad, CA) according to the recommendations of the manufacturer. To minimize variation, all RNA samples from a single experiment were reverse-transcribed simultaneously. Reactions contained 1× Sybergreen Universal PCR Master Mix, 150 nM forward and reverse primers, and 1 μl of cDNA in a 50 μl reaction volume. Thermal cycling was performed using 40 cycles at 95°C for 15 seconds and 60°C for 1 minute. Amplicon size and reaction specificity were confirmed by 1.5% agarose gel electrophoresis. Each PCR was repeated three times with RNA samples isolated from three independent experiments, and the average median threshold cycle values were used for analysis. β1-Actin was used to normalize samples for comparison. Comparative C_T method was used, where the fold change was calculated by the arithmetic formula: 2^{-00C_T}.

Immunofluorescence

NMuMG and MCT cells were grown on glass coverslips (22 × 22 mm). At 80% confluency, NMuMG and MCT cells were treated with TGF-β1 and/or U0126 for 24 and 48 hours,

Table 1. Microarray Analysis of TGF-β1–Treated NMuMG Cells Shows Upregulation of Genes in the Erk Pathway.

Gene name	TGF-β1 treatment		
	1 hour	6 hours	24 hours
H-ras	1.39	1.57	2.50
N-ras	2.25	1.34	2.14
Raf1	0.84	1.66	1.47
MEK2	1.98	2.14	1.65
Erk1	1.73	3.22	2.22

The values shown are RNA expression ratios of cells treated and not treated with TGF-β1 (4 ng/ml) for 1, 6, or 24 hours, after background deduction and normalization. Values greater than 2.0 are indicative of an above two-fold upregulation of gene expression. Data were analyzed according to Xie et al. [16].

respectively, as described in the Materials and Methods section. After treatment, cells were washed three times with phosphate-buffered saline (PBS) and fixed. For ZO-1 and E-cadherin staining, cells were fixed with ice-cold methanol for 20 minutes; for F-actin staining, cells were fixed at room temperature (RT) with 4% paraformaldehyde in PBS and then permeabilized with 0.05% Triton X-100 for 10 minutes. Cells were washed three times in PBS after each antibody incubation hereafter. Cells were blocked with 3% nonfat dry milk in PBS for 60 minutes at RT, incubated for 60 minutes with primary antibodies diluted in 3% milk/PBS, incubated with biotinylated secondary antibodies for 1 hour at RT, and incubated with streptavidin-conjugated Cy3 for 1 hour at RT. F-actin was stained with Texas Red-X phalloidin (2 U/ml) for 20 minutes at RT after permeabilization. Cell nuclei were stained with 1 μg/ml Hoechst 33258 for 10 minutes at RT. Coverslips were mounted on 25 × 75 mm microslides (VWR Scientific, Bridgeport, NJ) using AquaPolyMount (Polysciences, Warrington, PA). Cell morphology was monitored and photographed using an inverted phase contrast microscope (Olympus CK40; Olympus American Inc., Melville, NY). Fluorescent images were captured using a Princeton Instruments cooled CCD digital camera (Princeton Scientific Instruments Inc., Mammouth Junction, NJ) from a Zeiss Axiophot upright microscope (Carl Zeiss, Jena, Germany). Images were processed using Image Pro Plus software (Media Cybernetics, Silver Spring, MD).

Immunoblot Analysis

Cells were incubated in serum-free medium for 24 hours and treated with TGF-β1 and/or U0126 in serum-free medium as described in the Cell Culture and Treatment section. Cells were lysed in buffer containing 50 mM HEPES pH 7.5, 150 mM NaCl, 0.2 mM sodium vanadate, 10% glycerol, 1% NP-40, 0.1% SDS, 5 mM PNPP (*p*-nitrophenyl phosphate di Tris salt), 5 mM β-glycerol phosphate, 5 mM EDTA, 1 mM EGTA, 10 nM microcystine, and 200 μM phenylmethylsulfonyl fluoride (PMSF). Tris buffered saline with Tween 20 (TBST) was TBS-supplemented with 0.2% Tween 20. TBS buffer contained 100 mM Tris–HCl pH 7.5 and 0.9% NaCl. Protein concentrations in cell lysates were determined by the Bradford method. Protein extracts (40 μg/lane) were separated by 10% SDS polyacrylamide gel electrophoresis (SDS-PAGE) and transferred to nitrocellulose membranes (100 V, 70 minutes). Membranes were blocked with 5% BSA in TBST for 1 hour at RT and then incubated with primary antibodies in 5% BSA in TBST for 2 hours at RT, followed by incubation with secondary antibodies for 1 hour at RT. Membranes were washed five times in TBST and immunoreactive bands were detected by enhanced chemiluminescence (ECL; Amersham Biosciences). Molecular weights were estimated by comparison with BenchMark Prestained Protein Ladder (Invitrogen).

Kinase Assays

Kinase assays to detect Erk1 activity were performed on NMuMG and MCT cells treated with TGF-β1 and/or U0126 as described in the Cell Culture and Treatment section. Protein extractions and determination of protein concentrations were described above. Soluble lysates (500 μg of protein) were incubated with 1.5 μg of Erk1 antibody with gentle rocking overnight at 4°C. As a negative control, nontreated cell lysates were incubated with 1.5 μg of rabbit IgG. Protein G Sepharose (30 μl) was added to each immunoprecipitation complex, and incubated at 4°C for 3 hours while gently rocking. Then the immune complexes were washed three times with lysis buffer, two times with kinase buffer (25 mmol/l Tris pH 7.5, 5 mmol/l β1-glycerolphosphate, 2 mmol/l dithiothreitol, 0.1 mmol/l Na_3VO_4, and 10 mmol/l $MgCl_2$), and resuspended in 40 μl of kinase buffer containing 5 μmol of ATP, 5 μCi of ^{32}P ATP, and 5 μg of myelin basic protein. The kinase reactions were initiated by incubation at 37°C for 30 minutes. After boiling for 5 minutes, samples were subjected to 12% SDS-PAGE (20 μl in each lane). The intensity of the identified bands was detected using a Fujifilm FLA-5000 phosphoimager (Fuji Photo Film Co. Ltd., Stamford, CT). Equal amounts of the samples were subjected to 12% SDS-PAGE and analyzed by immunoblotting with Erk1 antibodies to detect total Erk1.

Results

TGF-β1 Induced the Erk Signaling Pathway in NMuMG

Microarray analyses were performed on RNA from NMuMG cells treated with TGF-β1 for 1, 6, and 24 hours,

Table 2. Comparison of TGF-β1–Induced Gene Expression Fold Changes from Microarray Analysis and RT-PCR in NMuMG cells.

Genes	TGF-β1 (hours)	Microarray	RT-PCR
H-ras	24	2.5	No change
N-ras	1	2.25	2.48
	24	2.14	2.71
Raf1	1	No change	2.51
MEK2	6	2.14	2.52
Erk1	6	3.22	2.88
	24	2.22	2.34

The microarray values are taken from Table 1. Values greater than 2.0 are indicative of an over two-fold upregulation of gene expression. Values less than 2.0 are not shown. RT-PCR values are shown as fold change between TGF-β1–treated and nontreated cells. Each RT-PCR analysis was repeated three times with RNA samples isolated from three independent experiments and the average median threshold cycle values were used for comparison. β1-Actin was used to normalize RNA levels between samples.

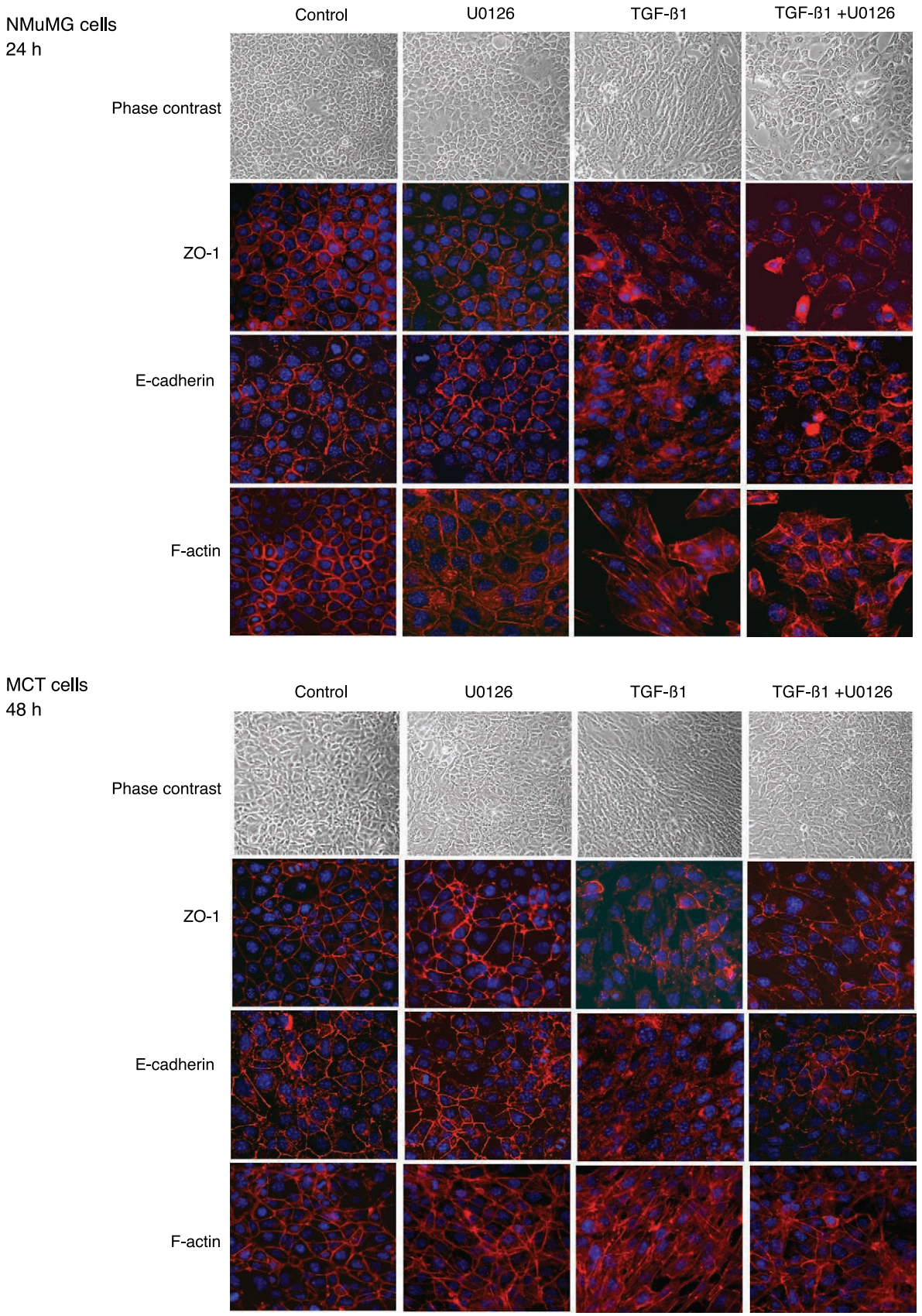

Figure 1. *Inhibition of TGF-β1–mediated EMT by the MEK inhibitor, U0126. NMuMG and MCT cells were treated with 4 ng/ml TGF-β1 in the absence or presence of 10 μM U0126 for 24 hours (NMuMG) or 48 hours (MCT). Nontreated cells or cells treated with U0126 alone were used as negative controls. Phase contrast images (×200) were captured to analyze cell morphology. Cells were stained for ZO-1, E-cadherin, and F-actin (red) and were counterstained with Hoechst 33258 (blue) to visualize cell nuclei. Immunofluorescent images were captured at ×400 magnification. Upon TGF-β1 treatment, cells elongated, ZO-1 and E-cadherin disappeared from cell junctions, and F-actin stress fibers formed. The MEK inhibitor (U0126) blocked these effects induced by TGF-β1.*

using a National Institute of Aging 15k cDNA set. Table 1 illustrates the expression levels of genes related to the Erk pathway upon treatment with TGF-β1 for 1, 6, and 24 hours. Values greater than 2.0 were indicative of an above two-fold upregulation of gene expression. Values less than 2.0 were not considered significant. H-ras (24 hours), N-ras (1 and 24 hours), MEK2 (6 hours), and Erk1 (6 and 24 hours) exhibited a greater than two-fold expression increase. Raf1 did not show an over two-fold significant increase in expression; however, it did show around a 1.5-fold expression increase (6 and 24 hours) (Table 1).

To verify the microarray data, RT-PCR was performed for the genes listed in Table 1. Table 2 compares the data generated by microarray analysis and RT-PCR on genes in the Erk pathway. Microarray and RT-PCR analyses showed similar trends of increased expression of Erk pathway genes in TGF-β1–treated NMuMG cells. However, the increased H-ras expression after 24 hours of TGF-β1 treatment was not confirmed by RT-PCR. Raf1 expression had a greater than two-fold increase by RT-PCR at 1 hour, but did not have increased expression by microarray analysis.

Activation of the Erk Signaling Pathway Was Required for TGF-β1–Induced EMT In Vitro

Results from microarray and RT-PCR analyses suggested that in NMuMG cells, the Erk signaling pathway may be activated by TGF-β1. Therefore, we investigated further the relationship between the Erk pathway and TGF-β1 signaling. The role of Erk activation in TGF-β1–induced EMT is unclear. To test whether Erk signaling was necessary for TGF-β1–induced EMT, Erk signaling was blocked using the MEK1/2 inhibitor, U0126. TGF-β1 induced EMT in NMuMG and MCT cells after 24 and 48 hours of TGF-β1 treatment, respectively (Figure 1). In the absence of treatment, NMuMG and MCT cells had an epithelial-like morphology with ZO-1, E-cadherin, and F-actin arranged in a cortical pattern at cell–cell junctions (Figure 1). Upon TGF-β1 treatment, phase contrast microscopy revealed that the cells underwent a morphologic change, from a cobblestone-like cell morphology to an elongated morphology. Immunofluorescence microscopy showed that the epithelial markers ZO-1 and E-cadherin disappeared from cell–cell junctions, and F-actin stress fibers formed after TGF-β1 treatment.

When NMuMG and MCT cells were treated with TGF-β1 in combination with the MEK1/2 inhibitor U0126 (TGF-β1 + U0126), the morphologic change induced by TGF-β1 alone was significantly blocked (Figure 1). The cobblestone-like appearance and junctional localization of ZO-1 and E-cadherin in the cells treated with TGF-β1 + U0126 remained intact. F-actin stress fiber formation was also attenuated in the cells treated with TGF-β1 + U0126. Treatment with U0126 alone did not change the morphology nor the localization of E-cadherin, ZO-1 and F-actin in the NMuMG and MCT cells. These data suggest that Erk signaling is necessary for TGF-β1–induced EMT in NMuMG and MCT cells.

TGF-β1 Increased Erk Phosphorylation in NMuMG and MCT

In Figure 2, the effects of U0126 on the activation of the Erk signaling pathway in NMuMG cells by TGF-β1 were studied by immunoblotting with total Raf1, phospho-MEK1/2, total MEK1/2, phospho-Erk1, and total Erk1 antibodies. Total Raf1 and phospho-Erk1 protein levels increased in NMuMG cells upon TGF-β1 treatment for 24 hours; however, these increases were blocked by cotreatment with U0126. Likewise, in MCT cells, phospho-Erk1 increased by TGF-β1

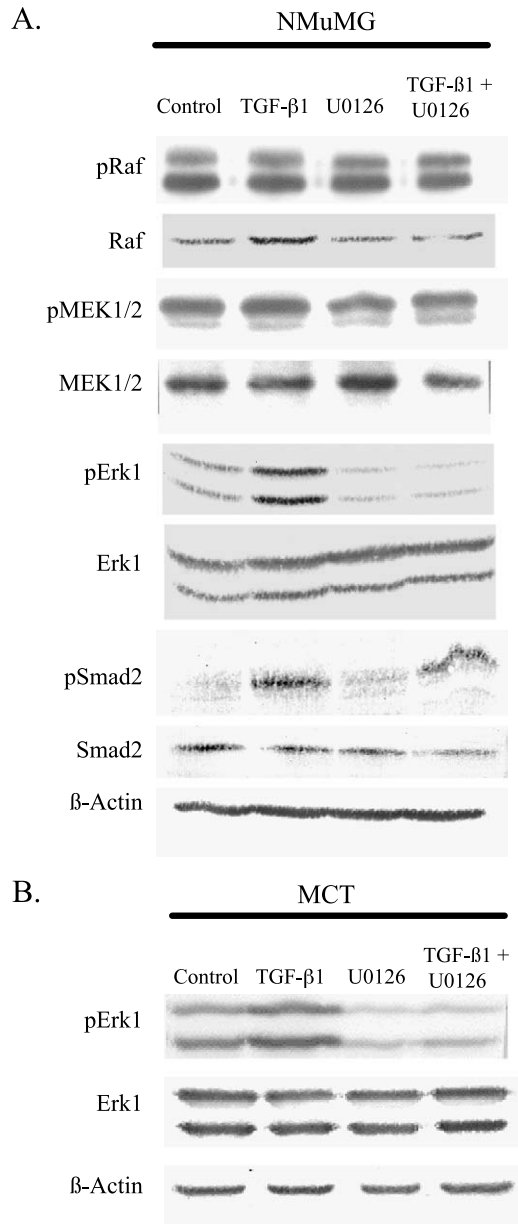

Figure 2. *U0126 blocks TGF-β1–induced phosphorylation of Erk. NMuMG (A) and MCT (B) cells were incubated with TGF-β1 (4 ng/ml) in the presence or absence of 10 μM U0126 for 24 hours. Cell lysates were analysed by SDS-PAGE and immunoblotted with antibodies to phospho-Raf, total Raf, phospho-MEK, total MEK, phospho-Erk, total Erk, phospho-Smad2, and total Smad2. β1-Actin was used as a control for equal protein loading. TGF-β1 treatment increased levels of phospho-Erk, and U0126 abolished this increase.*

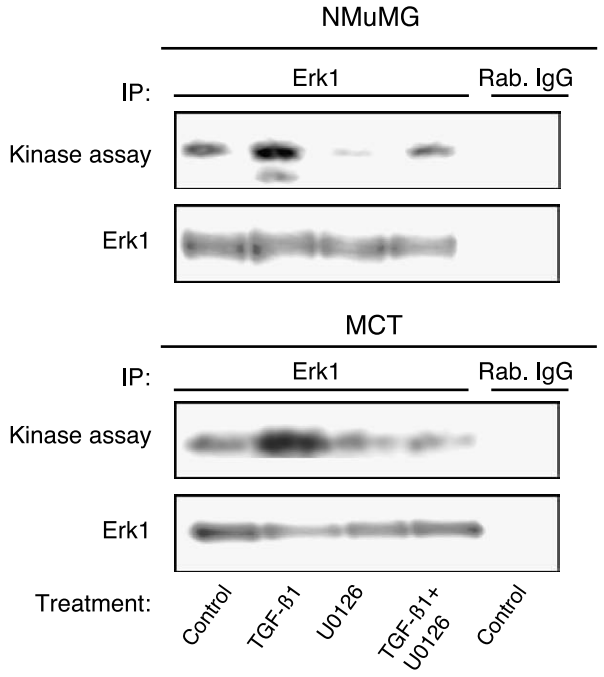

Figure 3. *U0126 blocks Erk kinase activity induced by TGF-β1. Erk kinase assays were performed on NMuMG and MCT cells treated with TGF-β1 (4 ng/ml) and/or U0126 (10 μM) for 24 hours. Nontreated cells were used as a control. Soluble lysates were immunoprecipitated with Erk1 antibody or rabbit IgG (Rab. IgG) as a control. The immunoprecipitates were subjected to immune complex kinase assays with myelin basic protein as the substrate. The kinase reactions or immunoprecipitates were analyzed by phosphorimaging and immunoblotting with Erk1. NMuMG and MCT cells treated with TGF-β1 had enhanced Erk activation. Treatment with U0126 reduced Erk kinase activity induced by TGF-β1.*

treatment, and this increase was abolished by U0126. Phospho-Smad2 protein levels increased after TGF-β1 treatment, and this increase was not blocked by U0126, indicating that U0126 did not inhibit TGF-β1 signaling through Smads. No changes were observed in phospho-Raf, phospho-MEK, total MEK, total Erk, or total Smad2 protein levels (Figure 2). β-Actin was used as control for equal protein loading.

MEK1/2 Inhibition Blocked TGF-β1–Induced Erk1 Activity

To assess Erk1 activity, Erk1 kinase assays were performed on cell lysates from NMuMG and MCT cells treated with TGF-β1 and/or U0126 for 24 hours (Figure 3). In both cell lines, TGF-β1 treatment induced Erk1 activity, whereas cotreatment with U0126 blocked the TGF-β1–mediated increase in Erk1 kinase activity. U0126 alone slightly decreased Erk1 activity. No kinase activity was detected in the rabbit IgG immunoprecipitation control. Immunoblotting with total Erk1 was used as a control for equal protein input in the immunoprecipitations.

Discussion

cDNA microarray analyses demonstrated an over two-fold increase in H-ras, N-ras, MEK2, and Erk1 gene expression in TGF-β1–treated NMuMG cells. RT-PCR confirmed most of these TGF-β1–induced gene expression changes. However, RT-PCR analyses did not confirm TGF-β1–induced changes in H-ras or Raf1 expression. The algorithms used to obtain the fold expression changes in RT-PCR and microarray analyses were not the same; therefore, the

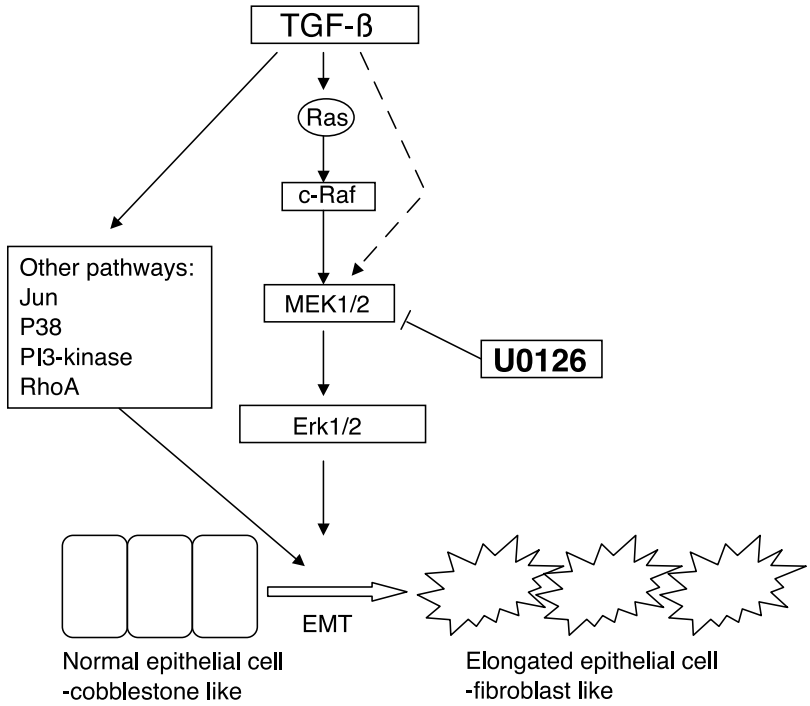

Figure 4. *Model of TGF-β1–induced Erk activation and EMT being blocked by U0126. TGF-β1 may activate the Erk pathway through upstream factors, such as Ras/Raf, or directly through more downstream factors, such as MEK or Erk. To investigate the role of Erk signaling in TGF-β1–mediated EMT, the MEK1/2 inhibitor, U0126, was used to block Erk phosphorylation in NMuMG and MCT cells. In these cells, TGF-β1 induction of Erk activity and EMT was blocked by U0126. However, TGF-β1 may activate other pathways, such as p38, JNK, PI3-kinase, and RhoA, to induce EMT in other cell types.*

fold changes observed between RT-PCR and microarray may not be identical. However, the patterns of expression determined by the two techniques were comparable.

Expression profiling at the mRNA level can provide important clues to the early changes in gene expression taking place in physiological or pathologic processes. Most genotypic changes are fundamentally manifest through changes in protein expression. Confirmation at the protein level was carried out after the microarray studies because protein expression levels are often not tightly correlated with RNA expression. As we determined subsequently, not all of the genes in the Erk pathway that exhibited upregulation at the RNA level in microarray analyses demonstrated an upregulation at the protein level.

The MEK1/2 inhibitor, U0126, was used to test whether the Erk signaling pathway was functionally involved in TGF-β1–induced EMT responses in NMuMG cells. Cultured mouse proximal tubular cells (MCT), which undergo TGF-β1–mediated EMT, were also used to determine if the Erk pathway was important in TGF-β1–mediated EMT. The fibroblast-like cell shape change induced by TGF-β1 was significantly blocked by U0126 in both cell lines. This morphologic change was accompanied by loss of ZO-1 and E-cadherin at cell–cell junctions, and the formation of actin stress fibers. After TGF-β1 plus U0126 treatment, NMuMG cells retained more ZO-1 and E-cadherin at cell–cell junctions than MCT cells. The inhibition of TGF-β1–induced stress fiber formation by U0126 was more evident in MCT cells than in NMuMG cells. Therefore, the importance of Erk signaling in TGF-β1–induced stress fibers and ZO-1 and E-cadherin redistribution may vary between cell lines. From our data, we conclude that activation of the Erk signaling pathway is required for TGF-β1–induced EMT *in vitro*. However, Erk signaling may not be solely responsible for TGF-β1–induced EMT because the blockage of EMT by U0126 in NMuMG and MCT cells was not complete. Levels of phosphorylated Smad2 increased after TGF-β1 treatment and remained elevated after TGF-β1 plus U0126 treatment of NMuMG cells. Therefore, U0126 did not block all TGF-β1 signaling and TGF-β1 may remain capable of activating other signaling pathways, such as the p38 MAPK, PI3k/Akt, and RhoA GTPase pathways, to induce EMT [8–10], as depicted in Figure 4.

The involvement of Erk signaling in TGF-β1–induced EMT is controversial [17, 18]. However, our data show that TGF-β1 may induce EMT *in vitro* through the activation of Erk1 without the requirement for oncogenic Ras. Phosphorylation of Raf1 was unaffected by treating NMuMG with TGF-β1 and/or U0126. Total Raf1 protein levels increased after TGF-β1 treatment but were unaffected by U0126. Interestingly, RT-PCR detected an upregulation of Raf1 gene expression after TGF-β1 treatment. However, levels of phosphorylated Erk1 and Erk1 kinase activity were increased after TGF-β1 treatment and these increases were blocked by U0126. Therefore, our data suggest that TGF-β1 may activate Erk1 to induce EMT *in vitro*.

Past reports have indicated that the ability of TGF-β1 to induce EMT may depend on the transformation state of the cell [18]. Many studies have shown a requirement for overexpression/mutational activation of elements of Ras/Raf/Erk for TGF-β1 –mediated EMT in human, rat, or mouse epidermal, pancreas, intestine, liver, prostate, and mammary epithelial cells [10,17–26]. Constitutive activation of Ras often leads to cellular transformation, and activation of mutations in the *ras* oncogenes occurs in a high proportion of human cancers [22,27–29]. Many carcinomas with activated *ras* oncogenes have undergone EMT [30–33]. In contrast, our data show that the Erk pathway is activated by TGF-β1 in two nontransformed cell lines NMuMG and MCT that undergo EMT, in the absence of oncogenic mutations in the Ras/Erk pathway; and that TGF-β1 activation of the Erk pathway is necessary for the induction of EMT. The observation that U0126 blocks TGF-β–induced Erk phosphorylation indicates that TGF-β activation of Erk is MEK-dependent.

TGF-β1–induced EMT has been implicated in pathologic states such as renal fibrosis and cancer. Our study is the first report to show that TGF-β1 can induce EMT through Erk activation in a cultured renal tubular cell line (MCT) [34–37]. In addition, many epithelial solid tumors become increasingly motile and invasive in response to TGF-β1. Therefore, selective inhibition of the Ras/Erk pathway may suppress TGF-β1–induced renal fibrosis and tumor invasion.

References

[1] Shi Y and Massague J (2003). Mechanisms of TGF-beta signaling from cell membrane to the nucleus. *Cell* **113,** 685–700.

[2] Massague J (1998). TGF-beta signal transduction. *Annu Rev Biochem* **67,** 753–791.

[3] de Caestecker MP, Piek E, and Roberts AB (2000). Role of transforming growth factor-beta signaling in cancer. *J Natl Cancer Inst* **92,** 1388–1402.

[4] Atfi A, Djelloul S, Chastre E, Davis R, and Gespach C (1997). Evidence for a role of Rho-like GTPases and stress-activated protein kinase/c-Jun N-terminal kinase (SAPK/JNK) in transforming growth factor beta–mediated signaling. *J Biol Chem* **272,** 1429–1432.

[5] Engel ME, McDonnell MA, Law BK, and Moses HL (1999). Interdependent SMAD and JNK signaling in transforming growth factor-beta–mediated transcription. *J Biol Chem* **274,** 37413–37420.

[6] Frey RS and Mulder KM (1997). Involvement of extracellular signal–regulated kinase 2 and stress-activated protein kinase/Jun N-terminal kinase activation by transforming growth factor beta in the negative growth control of breast cancer cells. *Cancer Res* **57,** 628–633.

[7] Hartsough MT and Mulder KM (1995). Transforming growth factor beta activation of p44MAPK in proliferating cultures of epithelial cells. *J Biol Chem* **270,** 7117–7124.

[8] Hanafusa H, Ninomiya-Tsuji J, Masuyama N, Nishita M, Fujisawa J, Shibuya H, Matsumoto K, and Nishida E (1999). Involvement of the p38 mitogen–activated protein kinase pathway in transforming growth factor-beta–induced gene expression. *J Biol Chem* **274,** 27161–27167.

[9] Bakin AV, Tomlinson AK, Bhowmick NA, Moses HL, and Arteaga CL (2000). Phosphatidylinositol 3-kinase function is required for transforming growth factor beta–mediated epithelial to mesenchymal transition and cell migration. *J Biol Chem* **275,** 36803–36810.

[10] Bhowmick NA, Ghiassi M, Bakin A, Aakre M, Lundquist CA, Engel ME, Arteaga CL, and Moses HL (2001). Transforming growth factor-beta1 mediates epithelial to mesenchymal transdifferentiation through a RhoA-dependent mechanism. *Mol Biol Cell* **12,** 27–36.

[11] Cereijido M, Shoshani L, and Contreras RG (2000). Molecular physiology and pathophysiology of tight junctions: I. Biogenesis of tight junctions and epithelial polarity. *Am J Physiol Gastrointest Liver Physiol* **279,** G477–G482.

[12] Grande M, Franzen A, Karlsson JO, Ericson LE, Heldin NE, and Nilsson M (2002). Transforming growth factor-beta and epidermal growth factor synergistically stimulate epithelial to mesenchymal transition (EMT) through a MEK-dependent mechanism in primary cultured pig thyrocytes. *J Cell Sci* **115,** 4227–4236.

[13] Miettinen PJ, Ebner R, Lopez AR, and Derynck R (1994). TGF-beta induced transdifferentiation of mammary epithelial cells to mesenchymal cells: involvement of type I receptors. *J Cell Biol* **127,** 2021–2036.

[14] Piek E, Moustakas A, Kurisaki A, Heldin CH, and ten Dijke P (1999). TGF-(beta) type I receptor/ALK-5 and Smad proteins mediate epithelial to mesenchymal transdifferentiation in NMuMG breast epithelial cells. *J Cell Sci* **112** (Part 24), 4557–4568.

[15] Zavadil J, Bitzer M, Liang D, Yang YC, Massimi A, Kneitz S, Piek E, and Bottinger EP (2001). Genetic programs of epithelial cell plasticity directed by transforming growth factor-beta. *Proc Natl Acad Sci USA* **98,** 6686–6691.

[16] Xie L, Law BK, Aakre ME, Edgerton M, Shyr Y, Bhowmick NA, and Moses HL (2003). Transforming growth factor beta–regulated gene expression in a mouse mammary gland epithelial cell line. *Breast Cancer Res* **5,** R187–R198.

[17] Ellenrieder V, Hendler SF, Boeck W, Seufferlein T, Menke A, Ruhland C, Adler G, and Gress TM (2001). Transforming growth factor beta1 treatment leads to an epithelial–mesenchymal transdifferentiation of pancreatic cancer cells requiring extracellular signal–regulated kinase 2 activation. *Cancer Res* **61,** 4222–4228.

[18] Janda E, Lehmann K, Killisch I, Jechlinger M, Herzig M, Downward J, Beug H, and Grunert S (2002). Ras and TGF[beta] cooperatively regulate epithelial cell plasticity and metastasis: dissection of Ras signaling pathways. *J Cell Biol* **156,** 299–313.

[19] Park BJ, Park JI, Byun DS, Park JH, and Chi SG (2000). Mitogenic conversion of transforming growth factor-beta1 effect by oncogenic Ha-Ras–induced activation of the mitogen-activated protein kinase signaling pathway in human prostate cancer. *Cancer Res* **60,** 3031–3038.

[20] Santibanez JF, Iglesias M, Frontelo P, Martinez J, and Quintanilla M (2000). Involvement of the Ras/MAPK signaling pathway in the modulation of urokinase production and cellular invasiveness by transforming growth factor-beta(1) in transformed keratinocytes. *Biochem Biophys Res Commun* **273,** 521–527.

[21] Oft M, Akhurst RJ, and Balmain A (2002). Metastasis is driven by sequential elevation of H-ras and Smad2 levels. *Nat Cell Biol* **4,** 487–494.

[22] Oft M, Peli J, Rudaz C, Schwarz H, Beug H, and Reichmann E (1996). TGF-β1 and Ha-Ras collaborate in modulating the phenotypic plasticity and invasiveness of epithelial tumor cells. *Genes Dev* **10,** 2462–2477.

[23] Gotzmann J, Huber H, Thallinger C, Wolschek M, Jansen B, Schulte-Hermann R, Beug H, and Mikulits W (2002). Hepatocytes convert to a fibroblastoid phenotype through the cooperation of TGF-β1 and Ha-Ras: steps towards invasiveness. *J Cell Sci* **115,** 1189–1202.

[24] Fujimoto K, Sheng H, Shao J, and Beauchamp RD (2001). Transforming growth factor-beta1 promotes invasiveness after cellular transformation with activated Ras in intestinal epithelial cells. *Exp Cell Res* **266,** 239–249.

[25] Oft M, Heider KH, and Beug H (1998). TGFbeta signaling is necessary for carcinoma cell invasiveness and metastasis. *Curr Biol* **8,** 1243–1252.

[26] Nicolas FJ, Lehmann K, Warne PH, Hill CS, and Downward J (2003). Epithelial mesenchymal transition in MDCK cells is accompanied by downregulation of Smad3 expression leading to resistance to TGFbeta–induced growth arrest. *J Biol Chem* **278,** 3251–3256.

[27] Fukuda M, Kurosaki W, Yanagihara K, Kuratsune H, and Sairenji T (2002). A mechanism in Epstein-Barr virus oncogenesis: inhibition of transforming growth factor-beta 1–mediated induction of MAPK/p21 by LMP1. *Virology* **302,** 310–320.

[28] Longstreet M, Miller B, and Howe PH (1992). Loss of transforming growth factor beta 1 (TGF-beta 1)–induced growth arrest and p34cdc2 regulation in ras-transfected epithelial cells. *Oncogene* **7,** 1549–1556.

[29] Coppa A, Mincione G, Lazzereschi D, Ranieri A, Turco A, Lucignano B, Scarpa S, Ragano-Caracciolo M, and Colletta G (1997). Restored expression of transforming growth factor beta type II receptor in k-ras–transformed thyroid cells, TGF beta-resistant, reverts their malignant phenotype. *J Cell Physiol* **172,** 200–208.

[30] Schoenenberger CA and Matlin KS (1991). Cell polarity and epithelial oncogenesis. *Trends Cell Biol* **1,** 87–92.

[31] Birchmeier W, Weidner KM, and Behrens J (1993). Molecular mechanisms leading to loss of differentiation and gain of invasiveness in epithelial cells. *J Cell Sci Suppl* **17,** 159–164.

[32] Hay ED and Zuk A (1995). Transformations between epithelium and mesenchyme: normal, pathological, and experimentally induced. *Am J Kidney Dis* **26,** 678–690.

[33] Hay ED (1995). An overview of epithelio-mesenchymal transformation. *Acta Anat (Basel)* **154,** 8–20.

[34] Wolf G, Ziyadeh FN, and Stahl RA (1999). Angiotensin II stimulates expression of transforming growth factor beta receptor type II in cultured mouse proximal tubular cells. *J Mol Med* **77,** 556–564.

[35] Weinreich T, Landolt M, Booy C, Wuthrich R, and Binswanger U (1999). 1,25-Dihydroxyvitamin D3 stimulates transforming growth factor-beta1 synthesis by mouse renal proximal tubular cells. *Kidney Blood Press Res* **22,** 99–105.

[36] Wolf G, Zahner G, Ziyadeh FN, and Stahl RA (1996). Cyclosporin A induces transcription of transforming growth factor beta in a cultured murine proximal tubular cell line. *Exp Nephrol* **4,** 304–308.

[37] Wolf G, Hannken T, Schroeder R, Zahner G, Ziyadeh FN, and Stahl RA (2001). Antioxidant treatment induces transcription and expression of transforming growth factor beta in cultured renal proximal tubular cells. *FEBS Lett* **488,** 154–159.

[38] Brown KA, Aakre ME, Gorska AE, Price JO, Eltom SE, Pietenpol JA, and Moses HL (2004). Induction by transforming growth factor-beta 1 of epithelial to mesenchymal transition is a rare event *in vitro*. *Breast Cancer Res* **6,** R215–R231.